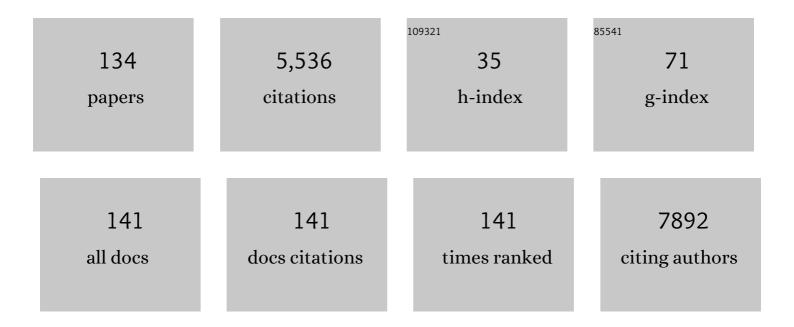
## Sarah E Bohndiek

List of Publications by Year in descending order

Source: https://exaly.com/author-pdf/7358621/publications.pdf Version: 2024-02-01



SARAH F ROHNDIEK

#	Article	IF	CITATIONS
1	Contrast agents for molecular photoacoustic imaging. Nature Methods, 2016, 13, 639-650.	19.0	979
2	Imaging biomarker roadmap for cancer studies. Nature Reviews Clinical Oncology, 2017, 14, 169-186.	27.6	792
3	Production of hyperpolarized [1,4- <sup>13</sup> C <sub>2</sub> ]malate from [1,4- <sup>13</sup> C <sub>2</sub> ]fumarate is a marker of cell necrosis and treatment response in tumors. Proceedings of the National Academy of Sciences of the United States of America, 2009, 106, 19801-19806.	7.1	328
4	Tumor imaging using hyperpolarized <sup>13</sup> C magnetic resonance spectroscopy. Magnetic Resonance in Medicine, 2011, 66, 505-519.	3.0	229
5	A small animal Raman instrument for rapid, wide-area, spectroscopic imaging. Proceedings of the National Academy of Sciences of the United States of America, 2013, 110, 12408-12413.	7.1	185
6	Hyperpolarized [1- <sup>13</sup> C]-Ascorbic and Dehydroascorbic Acid: Vitamin C as a Probe for Imaging Redox Status in Vivo. Journal of the American Chemical Society, 2011, 133, 11795-11801.	13.7	177
7	Detecting treatment response in a model of human breast adenocarcinoma using hyperpolarised [1-13C]pyruvate and [1,4-13C2]fumarate. British Journal of Cancer, 2010, 103, 1400-1406.	6.4	124
8	Magnetization transfer measurements of exchange between hyperpolarized [1- <sup>13</sup> C]pyruvate and [1- <sup>13</sup> C]lactate in a murine lymphoma. Magnetic Resonance in Medicine, 2010, 63, 872-880.	3.0	107
9	Molecular Photoacoustic Imaging of Follicular Thyroid Carcinoma. Clinical Cancer Research, 2013, 19, 1494-1502.	7.0	107
10	Magnetic resonance imaging with hyperpolarized [1,4- <sup>13</sup> C <sub>2</sub> ]fumarate allows detection of early renal acute tubular necrosis. Proceedings of the National Academy of Sciences of the United States of America, 2012, 109, 13374-13379.	7.1	99
11	Development and Application of Stable Phantoms for the Evaluation of Photoacoustic Imaging Instruments. PLoS ONE, 2013, 8, e75533.	2.5	94
12	Oxygen Enhanced Optoacoustic Tomography (OE-OT) Reveals Vascular Dynamics in Murine Models of Prostate Cancer. Theranostics, 2017, 7, 2900-2913.	10.0	83
13	A clinically translatable hyperspectral endoscopy (HySE) system for imaging the gastrointestinal tract. Nature Communications, 2019, 10, 1902.	12.8	75
14	Hyperpolarized 13C Spectroscopy Detects Early Changes in Tumor Vasculature and Metabolism after VEGF Neutralization. Cancer Research, 2012, 72, 854-864.	0.9	73
15	Towards Quantitative Evaluation of Tissue Absorption Coefficients Using Light Fluence Correction in Optoacoustic Tomography. IEEE Transactions on Medical Imaging, 2017, 36, 322-331.	8.9	73
16	Photoacoustic Tomography Detects Early Vessel Regression and Normalization During Ovarian Tumor Response to the Antiangiogenic Therapy Trebananib. Journal of Nuclear Medicine, 2015, 56, 1942-1947.	5.0	72
17	Photoacoustic imaging using genetically encoded reporters: a review. Journal of Biomedical Optics, 2017, 22, 070901.	2.6	72
18	Detection of Tumor Response to a Vascular Disrupting Agent by Hyperpolarized 13C Magnetic Resonance Spectroscopy. Molecular Cancer Therapeutics, 2010, 9, 3278-3288.	4.1	66

#	Article	IF	CITATIONS
19	Grayscale-to-Color: Scalable Fabrication of Custom Multispectral Filter Arrays. ACS Photonics, 2019, 6, 3132-3141.	6.6	65
20	Evaluation of Precision in Optoacoustic Tomography for Preclinical Imaging in Living Subjects. Journal of Nuclear Medicine, 2017, 58, 807-814.	5.0	64
21	Photoacoustic imaging as a tool to probe the tumour microenvironment. DMM Disease Models and Mechanisms, 2019, 12, .	2.4	57
22	Hyperpolarized <sup>13</sup> C MRI and PET: In Vivo Tumor Biochemistry. Journal of Nuclear Medicine, 2011, 52, 1333-1336.	5.0	52
23	A roadmap for the clinical implementation of optical-imaging biomarkers. Nature Biomedical Engineering, 2019, 3, 339-353.	22.5	52
24	Raman micro-spectroscopy for accurate identification of primary human bronchial epithelial cells. Scientific Reports, 2018, 8, 12604.	3.3	51
25	Empirical electroâ€optical and xâ€ray performance evaluation of CMOS active pixels sensor for low dose, high resolution xâ€ray medical imaging. Medical Physics, 2007, 34, 4612-4625.	3.0	49
26	Cellulose nanoparticles are a biodegradable photoacoustic contrast agent for use in living mice. Photoacoustics, 2014, 2, 119-127.	7.8	48
27	Comparison of Methods for Estimating the Conversion Gain of CMOS Active Pixel Sensors. IEEE Sensors Journal, 2008, 8, 1734-1744.	4.7	46
28	Analysis of image heterogeneity using 2D Minkowski functionals detects tumor responses to treatment. Magnetic Resonance in Medicine, 2014, 71, 402-410.	3.0	46
29	Optoacoustics delineates murine breast cancer models displaying angiogenesis and vascular mimicry. British Journal of Cancer, 2018, 118, 1098-1106.	6.4	44
30	Oxygen-Enhanced and Dynamic Contrast-Enhanced Optoacoustic Tomography Provide Surrogate Biomarkers of Tumor Vascular Function, Hypoxia, and Necrosis. Cancer Research, 2018, 78, 5980-5991.	0.9	44
31	ThX – a next-generation probe for the early detection of amyloid aggregates. Chemical Science, 2020, 11, 4578-4583.	7.4	43
32	Correlation of energy dispersive diffraction signatures and microCT of small breast tissue samples with pathological analysis. Physics in Medicine and Biology, 2007, 52, 6151-6164.	3.0	41
33	A non-free-space propagation x-ray phase contrast imaging method sensitive to phase effects in two directions simultaneously. Applied Physics Letters, 2009, 94, 044108.	3.3	41
34	A CMOS active pixel sensor system for laboratory- based x-ray diffraction studies of biological tissue. Physics in Medicine and Biology, 2008, 53, 655-672.	3.0	40
35	Deep learning applied to hyperspectral endoscopy for online spectral classification. Scientific Reports, 2020, 10, 3947.	3.3	37
36	Learned spectral decoloring enables photoacoustic oximetry. Scientific Reports, 2021, 11, 6565.	3.3	34

#	Article	IF	CITATIONS
37	Characterizing Optical Fiber Transmission Matrices Using Metasurface Reflector Stacks for Lensless Imaging without Distal Access. Physical Review X, 2019, 9, .	8.9	33
38	Assessing Oxidative Stress in Tumors by Measuring the Rate of Hyperpolarized [1-13C]Dehydroascorbic Acid Reduction Using 13C Magnetic Resonance Spectroscopy. Journal of Biological Chemistry, 2017, 292, 1737-1748.	3.4	32
39	An Activatable Cancer-Targeted Hydrogen Peroxide Probe for Photoacoustic and Fluorescence Imaging. Cancer Research, 2019, 79, 5407-5417.	0.9	31
40	Fluorescence hyperspectral imaging (fHSI) using a spectrally resolved detector array. Journal of Biophotonics, 2017, 10, 840-853.	2.3	29
41	Characterization and Testing of LAS: A Prototype `Large Area Sensor' With Performance Characteristics Suitable for Medical Imaging Applications. IEEE Transactions on Nuclear Science, 2009, 56, 2938-2946.	2.0	26
42	Label-free monitoring of tissue biochemistry following traumatic brain injury using Raman spectroscopy. Analyst, The, 2017, 142, 132-139.	3.5	26
43	Improving Image Quality by Accounting for Changes in Water Temperature during a Photoacoustic Tomography Scan. PLoS ONE, 2012, 7, e45337.	2.5	25
44	Optoacoustic Detection of Early Therapy-Induced Tumor Cell Death Using a Targeted Imaging Agent. Clinical Cancer Research, 2017, 23, 6893-6903.	7.0	25
45	Characterization studies of two novel active pixel sensors. Optical Engineering, 2007, 46, 124003.	1.0	23
46	Design and validation of a near-infrared fluorescence endoscope for detection of early esophageal malignancy. Journal of Biomedical Optics, 2016, 21, 084001.	2.6	23
47	Imaging and â€~omic' methods for the molecular diagnosis of cancer. Expert Review of Molecular Diagnostics, 2010, 10, 417-434.	3.1	22
48	Development of a blood oxygenation phantom for photoacoustic tomography combined with online pO2 detection and flow spectrometry. Journal of Biomedical Optics, 2019, 24, 1.	2.6	22
49	Signal and noise transfer properties of CMOS based active pixel flat panel imager coupled to structured CsI:Tl. Medical Physics, 2009, 36, 116-126.	3.0	21
50	Detection of early neoplasia in Barrett's esophagus using lectin-based near-infrared imaging: an ex vivo study on human tissue. Endoscopy, 2018, 50, 618-625.	1.8	21
51	Co-registration of optoacoustic tomography and magnetic resonance imaging data from murine tumour models. Photoacoustics, 2020, 18, 100147.	7.8	21
52	Addressing photoacoustics standards. Nature Photonics, 2019, 13, 298-298.	31.4	20
53	A Comparative Photophysical Study of Structural Modifications of Thioflavin T-Inspired Fluorophores. Journal of Physical Chemistry Letters, 2020, 11, 8406-8416.	4.6	20
54	Criteria for the design of tissue-mimicking phantoms for the standardization of biophotonic instrumentation. Nature Biomedical Engineering, 2022, 6, 541-558.	22.5	20

#	Article	IF	CITATIONS
55	First evidence of phase-contrast imaging with laboratory sources and active pixel sensors. Nuclear Instruments and Methods in Physics Research, Section A: Accelerators, Spectrometers, Detectors and Associated Equipment, 2007, 581, 776-782.	1.6	19
56	Evaluation of illumination system uniformity for wide-field biomedical hyperspectral imaging. Journal of Optics (United Kingdom), 2017, 19, 045301.	2.2	19
57	Current and Emerging Technologies for Probing Molecular Signatures of Traumatic Brain Injury. Frontiers in Neurology, 2017, 8, 450.	2.4	18
58	Graphitic and oxidised high pressure high temperature (HPHT) nanodiamonds induce differential biological responses in breast cancer cell lines. Nanoscale, 2018, 10, 12169-12179.	5.6	17
59	Bimodal reflectance and fluorescence multispectral endoscopy based on spectrally resolving detector arrays. Journal of Biomedical Optics, 2018, 24, 1.	2.6	17
60	A CMOS Image Sensor With In-Pixel ADC, Timestamp, and Sparse Readout. IEEE Sensors Journal, 2009, 9, 20-28.	4.7	16
61	Quantitative phase and polarization imaging through an optical fiber applied to detection of early esophageal tumorigenesis. Journal of Biomedical Optics, 2019, 24, 1.	2.6	16
62	Distance dependent photoacoustics revealed through DNA nanostructures. Nanoscale, 2017, 9, 16193-16199.	5.6	15
63	Emerging optical methods for endoscopic surveillance of Barrett's oesophagus. The Lancet Gastroenterology and Hepatology, 2018, 3, 349-362.	8.1	15
64	Spectral Endoscopy Enhances Contrast for Neoplasia in Surveillance of Barrett's Esophagus. Cancer Research, 2021, 81, 3415-3425.	0.9	14
65	Photoacoustics resolves species-specific differences in hemoglobin concentration and oxygenation. Journal of Biomedical Optics, 2020, 25, .	2.6	14
66	Full-field quantitative phase and polarisation-resolved imaging through an optical fibre bundle. Optics Express, 2019, 27, 23929.	3.4	14
67	Characterisation of Vanilla—A novel active pixel sensor for radiation detection. Nuclear Instruments and Methods in Physics Research, Section A: Accelerators, Spectrometers, Detectors and Associated Equipment, 2007, 581, 287-290.	1.6	13
68	Optical characterisation of a CMOS active pixel sensor using periodic noise reduction techniques. Nuclear Instruments and Methods in Physics Research, Section A: Accelerators, Spectrometers, Detectors and Associated Equipment, 2010, 620, 549-556.	1.6	13
69	Quantitation of a spin polarizationâ€induced nuclear Overhauser effect (SPINOE) between a hyperpolarized 13 Câ€labeled cell metabolite and water protons. Contrast Media and Molecular Imaging, 2014, 9, 182-186.	0.8	13
70	Quantification of vascular networks in photoacoustic mesoscopy. Photoacoustics, 2022, 26, 100357.	7.8	13
71	The Multidimensional Integrated Intelligent Imaging project (MI-3). Nuclear Instruments and Methods in Physics Research, Section A: Accelerators, Spectrometers, Detectors and Associated Equipment, 2009, 604, 196-198.	1.6	12
72	Reconstruction of Optical Vector-Fields With Applications in Endoscopic Imaging. IEEE Transactions on Medical Imaging, 2019, 38, 955-967.	8.9	12

#	Article	IF	CITATIONS
73	An active pixel sensor x-ray diffraction (APXRD) system for breast cancer diagnosis. Physics in Medicine and Biology, 2009, 54, 3513-3527.	3.0	11
74	Characterisation of regional variations in a stitched CMOS active pixel sensor. Nuclear Instruments and Methods in Physics Research, Section A: Accelerators, Spectrometers, Detectors and Associated Equipment, 2010, 620, 540-548.	1.6	11
75	Bifunctional fluorescent probes for detection of amyloid aggregates and reactive oxygen species. Royal Society Open Science, 2018, 5, 171399.	2.4	11
76	Opti-MSFA: a toolbox for generalized design and optimization of multispectral filter arrays. Optics Express, 2022, 30, 7591.	3.4	11
77	The Potential of Photoacoustic Imaging in Radiation Oncology. Frontiers in Oncology, 2022, 12, 803777.	2.8	11
78	Photoacoustic Tomography Detects Response and Resistance to Bevacizumab in Breast Cancer Mouse Models. Cancer Research, 2022, 82, 1658-1668.	0.9	11
79	Coherent Imaging Through Multicore Fibres With Applications in Endoscopy. Journal of Lightwave Technology, 2019, 37, 5733-5745.	4.6	10
80	A Copolymer-in-Oil Tissue-Mimicking Material With Tuneable Acoustic and Optical Characteristics for Photoacoustic Imaging Phantoms. IEEE Transactions on Medical Imaging, 2021, 40, 3593-3603.	8.9	10
81	First experience in clinical application of hyperspectral endoscopy for evaluation of colonic polyps. Journal of Biophotonics, 2021, 14, e202100078.	2.3	10
82	Hyperspectral imaging in biomedical applications. Journal of Optics (United Kingdom), 2019, 21, 010202.	2.2	9
83	Technical validation studies of a dual-wavelength LED-based photoacoustic and ultrasound imaging system. Photoacoustics, 2021, 22, 100267.	7.8	9
84	SIMPA: an open-source toolkit for simulation and image processing for photonics and acoustics. Journal of Biomedical Optics, 2022, 27, .	2.6	9
85	Smartâ€Dustâ€Nanorice for Enhancement of Endogenous Raman Signal, Contrast in Photoacoustic Imaging, and T2â€Shortening in Magnetic Resonance Imaging. Small, 2018, 14, e1703683.	10.0	8
86	Optoacoustic Imaging Detects Hormone-Related Physiological Changes of Breast Parenchyma. Ultraschall in Der Medizin, 2019, 40, 757-763.	1.5	8
87	Quantitative evaluation of comb-structure correction methods for multispectral fibrescopic imaging. Scientific Reports, 2018, 8, 17801.	3.3	7
88	First-in-human pilot study of snapshot multispectral endoscopy for early detection of Barrett's-related neoplasia. Journal of Biomedical Optics, 2021, 26, .	2.6	7
89	A 54mm x 54mm — 1.8Megapixel CMOS image sensor for medical imaging. , 2008, , .		6
90	An active DNA-based nanoprobe for photoacoustic pH imaging. Chemical Communications, 2018, 54, 10176-10178.	4.1	6

#	Article	IF	CITATIONS
91	A background correction method to compensate illumination variation in hyperspectral imaging. PLoS ONE, 2020, 15, e0229502.	2.5	6
92	The IPASC data format: A consensus data format for photoacoustic imaging. Photoacoustics, 2022, 26, 100339.	7.8	6
93	Single-Pixel Phase-Corrected Fiber Bundle Endomicroscopy With Lensless Focussing Capability. Journal of Lightwave Technology, 2015, 33, 3419-3425.	4.6	5
94	DNAâ€Based Nanocarriers to Enhance the Optoacoustic Contrast of Tumors In Vivo. Advanced Healthcare Materials, 2021, 10, e2001739.	7.6	5
95	Evaluation of Label-Free Confocal Raman Microspectroscopy for Monitoring Oxidative Stress In Vitro in Live Human Cancer Cells. Antioxidants, 2022, 11, 573.	5.1	5
96	Hyperspectral fluorescence imaging with multi wavelength LED excitation. Proceedings of SPIE, 2016, ,	0.8	4
97	Towards a simulation framework to maximize the resolution of biomedical hyperspectral imaging. Proceedings of SPIE, 2017, , .	0.8	4
98	Optical and x-ray characterization of two novel CMOS image sensors. , 2007, , .		3
99	A multispectral endoscope based on spectrally resolved detector arrays. Proceedings of SPIE, 2017, , .	0.8	3
100	Multi-modal imaging of high-risk ductal carcinoma in situ of the breast using C2Am: a targeted cell death imaging agent. Breast Cancer Research, 2021, 23, 25.	5.0	3
101	Nanodiamond preparation and surface characterization for biological applications. Proceedings of SPIE, 2017, , .	0.8	2
102	Light fluence correction for quantitative determination of tissue absorption coefficient using multi-spectral optoacoustic tomography. , 2015, , .		2
103	Spectrally tailored 'hyperpixel' filter arrays for imaging of chemical compositions. , 2022, , .		2
104	Development of a prototype sensor system for ultra-high-speed LDA-PIV. , 2008, , .		1
105	Stable phantoms for characterization of photoacoustic tomography (PAT) systems. Proceedings of SPIE, 2013, , .	0.8	1
106	Cellulose nanoparticles: photoacoustic contrast agents that biodegrade to simple sugars. Proceedings of SPIE, 2014, , .	0.8	1
107	Gold nanorods combine photoacoustic and Raman imaging for detection and treatment of ovarian cancer. , 2014, , .		1
108	Evaluation of multispectral optoacoustic tomography (MSOT) performance in phantoms and in vivo. , 2015, , .		1

#	Article	IF	CITATIONS
109	Experimental evaluation of a hyperspectral imager for near-infrared fluorescent contrast agent studies. Proceedings of SPIE, 2015, , .	0.8	1
110	Measurement of changes in blood oxygenation using Multispectral Optoacoustic Tomography (MSOT) allows assessment of tumor development. , 2016, , .		1
111	Spectral band optimization for multispectral fluorescence imaging. , 2017, , .		1
112	Evaluation of illumination systems for wide-field hyperspectral imaging in biomedical applications. , 2017, , .		1
113	Twelve tips for engaging with biologists, as told by a physicist. Nature, 2020, 577, 283-284.	27.8	1
114	IPASC: a Community-Driven Consensus-Based Initiative Towards Standardisation in Photoacoustic Imaging. , 2020, , .		1
115	Application of confocal Raman micro-spectroscopy for label-free monitoring of oxidative stress in living bronchial cells. , 2018, , .		1
116	Abstract 4198: Optoacoustic imaging of blood vasculature and study of angiogenesis in orthotopic breast cancer models. Cancer Research, 2016, 76, 4198-4198.	0.9	1
117	Robustness to misalignment of low-cost, compact quantitative phase imaging architectures. OSA Continuum, 2020, 3, 2660.	1.8	1
118	Curriculum blues. Physics World, 2002, 15, 18-18.	0.0	0
119	The good mentorship guide. Physics World, 2013, 26, 44-45.	0.0	0
120	Light fluence correction for quantitative determination of tissue absorption coefficient using multi-spectral optoacoustic tomography. , 2015, , .		0
121	In vivo light fluence correction for determination of tissue absorption coefficient using Multispectral Optoacoustic Tomography. , 2016, , .		0
122	Design and validation of a near-infrared fluorescence endoscope for detection of early esophageal malignancy using a targeted imaging probe. Proceedings of SPIE, 2016, , .	0.8	0
123	Quantitative imaging of tumor vasculature using multispectral optoacoustic tomography (MSOT). , 2017, , .		0
124	Tolerancing the alignment of large-core optical fibers, fiber bundles and light guides using a Fourier approach. Applied Optics, 2017, 56, 3303.	1.8	0
125	Abstract 2047: Molecular photoacoustic imaging and serum diagnostics rapidly detect response to angiopoietin 1 and 2 blockade in ovarian cancer. , 2014, , .		0
126	Abstract 2866: Volumetric optoacoustic imaging of tumor cell death using a targeted imaging agent. , 2017, , .		0

#	Article	IF	CITATIONS
127	Wide-field phase imaging for the endoscopic detection of dysplasia and early-stage esophageal cancer. , 2018, , .		0
128	Optimizing achromaticity in metalenses, and development of a layered thin-film metalens. , 2022, , .		0
129	A background correction method to compensate illumination variation in hyperspectral imaging. , 2020, 15, e0229502.		О
130	A background correction method to compensate illumination variation in hyperspectral imaging. , 2020, 15, e0229502.		0
131	A background correction method to compensate illumination variation in hyperspectral imaging. , 2020, 15, e0229502.		Ο
132	A background correction method to compensate illumination variation in hyperspectral imaging. , 2020, 15, e0229502.		0
133	A background correction method to compensate illumination variation in hyperspectral imaging. , 2020, 15, e0229502.		Ο
134	A background correction method to compensate illumination variation in hyperspectral imaging. , 2020, 15, e0229502.		0